JOURNAL OF MATERIALS SCIENCE 28 (1993) 415–422

Compositional variations in the bulk of $YBa_2Cu_3O_x$ thick films

D. K. ASWAL, S. K. GUPTA, S. C. SABHARWAL, M. K. GUPTA
Technical Physics and Prototype Engineering Division, Bhabha Atomic Research Centre, Trombay, Bombay 400 085, India

Thick films of $YBa_2Cu_3O_x$ (123) prepared on a number of substrate materials, namely Si, Al_2O_3, $SrTiO_3$, MgO and YSZ, have been investigated for the compositional variations/impurity phases present, microstructure, grain orientation etc. Energy-dispersive X-ray and X-ray diffraction analyses for as-prepared films of two different thicknesses, 2–3 μm and 10–15 μm, and after their partial and complete etching, are reported. The results show that the film–substrate reaction dominates up to ~2–3 μm thickness of a film. The decomposition of 123 material at the processing temperature and the substrate–film reaction together are seen to govern the crystallization behaviour, compositional variations and the superconducting properties of the films. In various cases, the films have been found to undergo superconducting phase transitions at temperatures between 66 and 89.5 K.

1. Introduction

We recently reported [1] on the preparation of both undoped and Ag-doped thick films of $YBa_2Cu_3O_x$ (123) on (100) $SrTiO_3$ substrates. In the case of undoped films, it was found essential to process the painted material above its partial melting temperature in order to obtain good adhesion characteristics. Energy-dispersive X-ray analysis (EDAX) of these samples showed the presence of $BaCuO_2$ on the film surface, indicating the decomposition of 123 material. This result also suggests that other products of 123 decomposition must be getting segregated from the top of the film towards the film–substrate interface. Our recent experiments have shown that the distribution of the products of decomposition within the film volume, besides other factors, is governed by the reaction processes occurring at the film–substrate interface. In the present communication we discuss the results of this investigation. In the study carried out, films prepared on a number of substrates, namely, Si, $SrTiO_3$, Al_2O_3, MgO and YSZ, were employed. From the results of our EDAX and X-ray diffraction (XRD) measurements, schematic diagrams showing the compositions of different regions of the films are obtained. It may be mentioned that a number of investigations related to the film–substrate reaction [2–6] or the decomposition of 123 [7–9] have been separately reported in the literature. However, the changes occurring in the bulk of a film due to a combined effect of the above two factors have not been investigated so far. The microstructures of the films prepared were studied by scanning electron microscopy. The results show that except for the films which were prepared using Si substrates, a liquid-assisted crystallization is observed to take place.

2. Experimental procedure

Thick films were prepared by the paint-on method using an ink of stoichiometric 123 material. For the preparation of the ink, 123 powder was synthesized in the usual manner by sintering the powder of the constituent oxides/carbonates mixed in their stoichiometric ratios. The synthesized powder was mixed with isopropyl alcohol and the drops of ink were applied on to a substrate. After the applied material was dried at room temperature, the painted material was subjected to a thermal treatment between 940 and 1050 °C

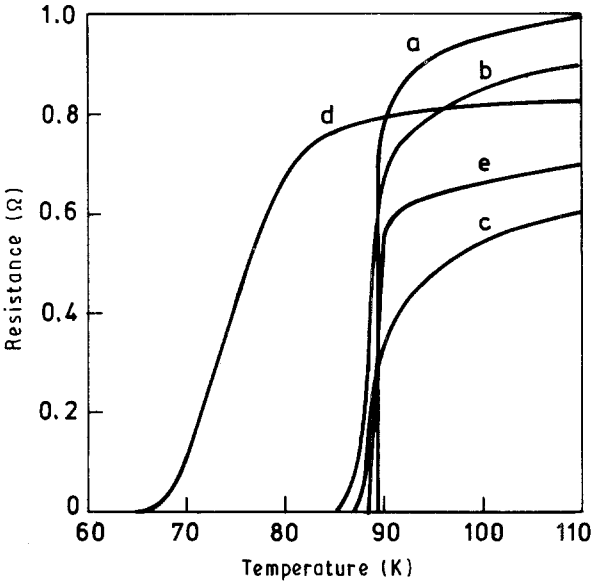

Figure 1 Temperature dependence of the resistance for films on different substrates: (a) Si, (b) Al_2O_3, (c) $SrTiO_3$, (d) MgO and (e) YSZ. Film thickness ~15 μm.

0022–2461 © *1993 Chapman & Hall*

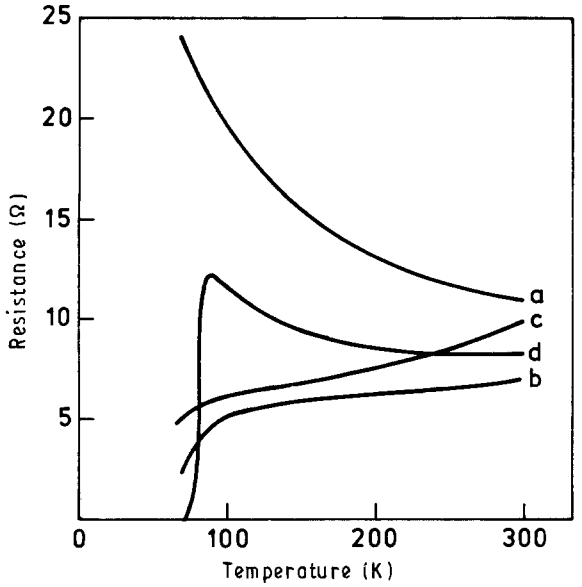

Figure 2 Resistance versus temperature plots for 2–3 μm thick films on different substrates: (a) Al_2O_3, (b) $SrTiO_3$, (c) MgO and (d) YSZ.

TABLE I Results of EDAX analysis

Substrate	Film sample[a]	Composition (at. frac.)			Substrate element
		Y	Ba	Cu	
Si	1	1	1.96	2.98	
	2	1	1.40	2.81	
	3	0.0	1.47	0.17	Si (98.3%)
Al_2O_3	1	1	2.32	3.81	
	2	1	2.79	4.54	
	3	1.64	0.14	0.11	Al (98.11%)
$SrTiO_3$	1	1	1.79	2.95	
	2	1	1.53	2.81	
	3	–	–	–	
MgO	1	1	2.0	2.98	
	2	1	2.1	3.01	
	3	–	–	–	Mg (100%)
YSZ	1	1	2.07	3.11	
	2	1	1.86	2.89	
	3	8.4	0.4	–	Zr (91.2%)

[a] Sample 1: as-prepared, sample 2: partially etched, sample 3: fully etched.

under flowing oxygen conditions. Films having thicknesses in the ranges 2–3 μm, 10–15 μm and those above 50 μm were prepared. The film thickness could be controlled through the adjustment of the ink viscosity. While the films having a thickness less than 50 μm had a smooth surface, for thicker ones blistering was observed. XRD for phase identification, scanning electron microscopy for the assessment of void density and grain size and EDAX for the chemical composition were carried out for the films prepared. The temperature dependence of film resistance was measured by the usual four-probe technique.

3. Results and discussion

Films were prepared using substrates of different materials, namely Si, Al_2O_3, $SrTiO_3$, MgO and YSZ. In the preparatory method followed, the painted samples were introduced directly into the hot zone of a tubular furnace preset at a given temperature for the thermal treatment. However, after the thermal treatment, films were brought down to room temperature at different rates. For the films which were 2–3 μm thick, irrespective of the cooling rate used, poor superconducting properties were measured. For the films of intermediate thickness in the range 10–15 μm, the best

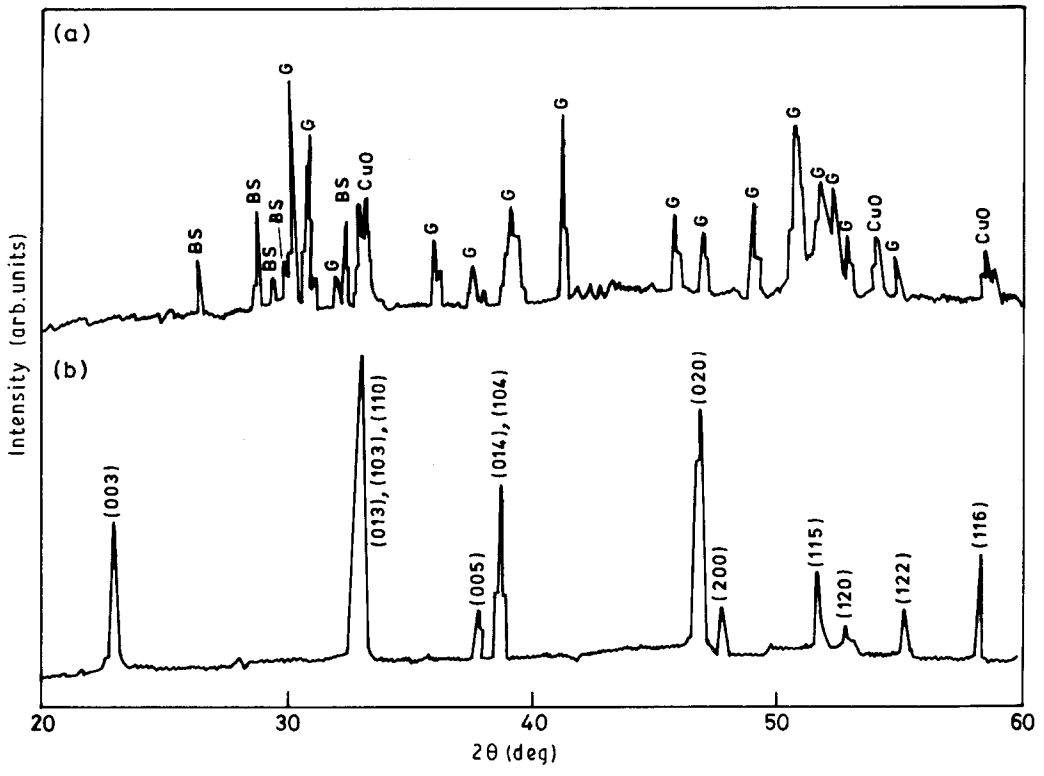

Figure 3 X-ray diffraction patterns recorded for (a) 2–3 μm (thin) and (b) 10–15 μm (thick) films on silicon. G = Y_2BaCuO_5, BS = Ba_2SiO_4.

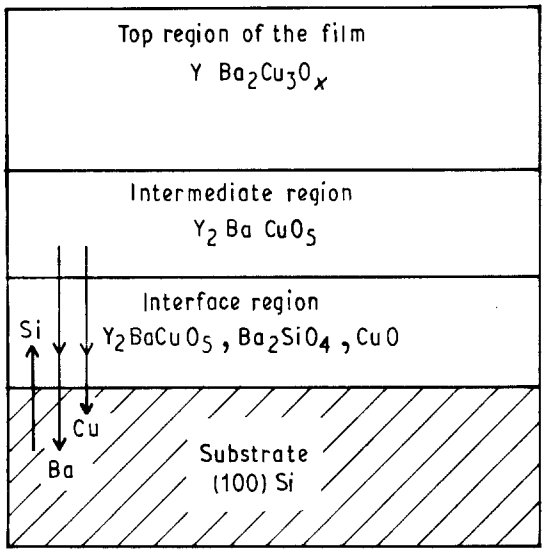

Figure 4 Schematic diagram showing the compositions of the different regions of a film on Si.

superconducting properties were obtained for films which were fast-cooled from the processing temperature to 750 °C in the first step and thereafter to room temperature at a slower rate. The resistance versus temperature plots obtained for such films are shown in Fig. 1. For comparison, similar plots for thinner films (2–3 μm thickness) prepared using an identical thermal cycle are shown in Fig. 2. It may be mentioned that thinner films on Si substrates were always found to be insulating, whereas those prepared on other substrates showed either semiconductor or metal-like behaviour depending upon the substrate material. In the case of films of intermediate thickness, fast cooling from the processing temperature was found essential to achieve superconductivity [1].

In order to investigate the reaction processes taking place at the interface, in different experiments the samples of intermediate thickness were etched down to 2–3 μm thickness and in others completely. The etching was carried out using dilute HNO_3. The results of EDAX for the as-prepared, partially etched as well as completely etched samples are given in Table I. It should be mentioned here that the composition of the partially etched and that of the as-prepared 2–3 μm thick films on various substrates were found to be essentially the same. It is therefore reasonable to assume that the XRD of a thinner film is representative of the interface reaction. The results of the film–substrate interaction for films on different substrates are described below.

3.1. Silicon substrate

The composition of an as-prepared film, as may be seen from Table I, corresponds to that of the starting material used for its preparation. However, a partially etched film is found to be deficient in Ba and Cu, the Ba deficiency being larger than that of Cu In the case of a fully etched film, the substrate surface is found to be contaminated by Ba and Cu. The amount of Ba in this case is far more than the Cu. The results clearly suggest that the diffusion of Ba from the film into the substrate is higher than that of Cu. X-ray diffraction patterns obtained for an as-prepared film and the

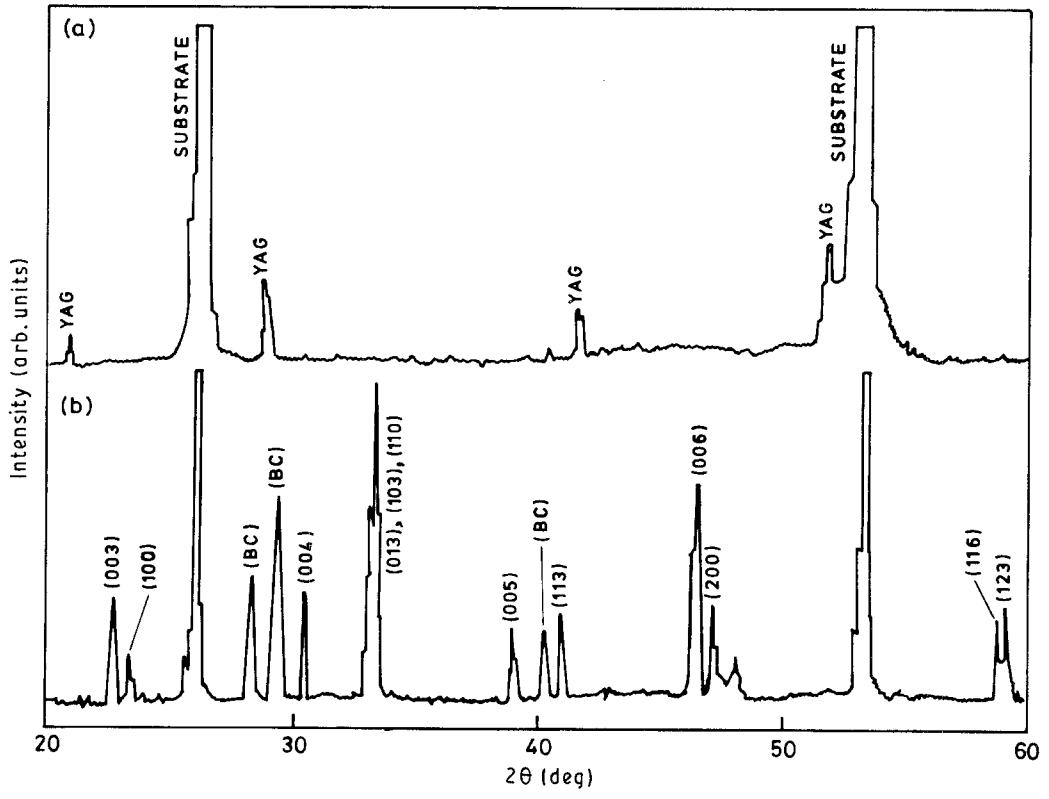

Figure 5 XRD patterns obtained for films on alumina: (a) substrate after etching and (b) ~15 μm thick film. YAG = $Y_3Al_5O_{12}$, BC = $BaCuO_2$.

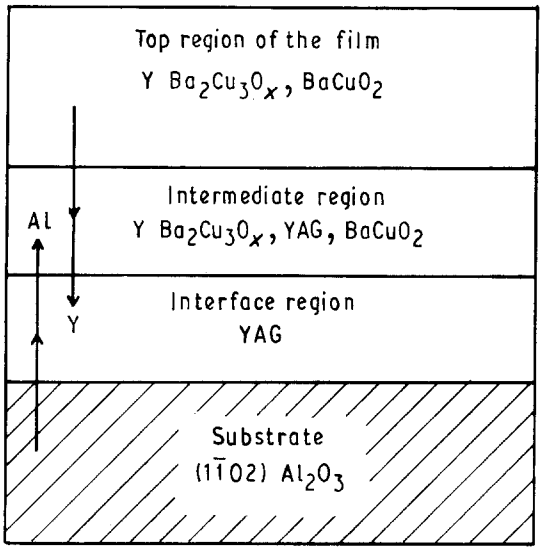

Figure 6 Schematic diagram showing the compositions of the different regions of a film on alumina.

interface region and reproduced in Fig. 3 also confirm this. The data reveal the formation of pure 123 phase in the former case. However, in the latter case, while the presence of Y_2BaCuO_5, Ba_2SiO_4 and CuO is seen, the reflections due to the 123 phase are completely missing. Further, as would be expected, the interface region is found to be electrically insulating while an as-prepared film undergoes a superconducting transition at 89.5 K according to plot (a) in Fig. 1.

The reaction products formed in the particular case are schematically shown in Fig. 4. The formation of a layer of 211 phase above the interface is thought to act as a buffer between the interface and the 123 film. The formation of Ba_2SiO_4 at the interface in this case is also reported in the literature [3, 4, 10].

3.2. Sapphire substrate

From the results of the EDAX measurements for films on Al_2O_3 shown in Table I, it is seen that yttrium from the bulk of the film diffuses into the substrate. This is also confirmed by the XRD recorded for both as-prepared and fully etched films shown in Fig. 5. From these plots it is found that the top of a film is rich in $BaCuO_2$, while at the interface region the formation of $Y_3Al_5O_{12}$ (YAG) takes place. This explains the observed differences in the resistivity behaviours of both thick and thin films as shown in Figs 1b and 2a. From the data obtained for the compositions of as-prepared, partially and fully etched films, a schematic diagram showing compositions of different regions of the film is shown in Fig. 6. Earlier reports have shown that the top of a film on sapphire is slightly rich in $BaCuO_2$ [11, 12]. The present study shows that this is because of the diffusion of yttrium towards the interface. In some cases the formation of Al_2BaO_4 at the interface has also been reported [3, 4, 13]. The reason for this is traced to the difference in the film processing temperatures in the two cases.

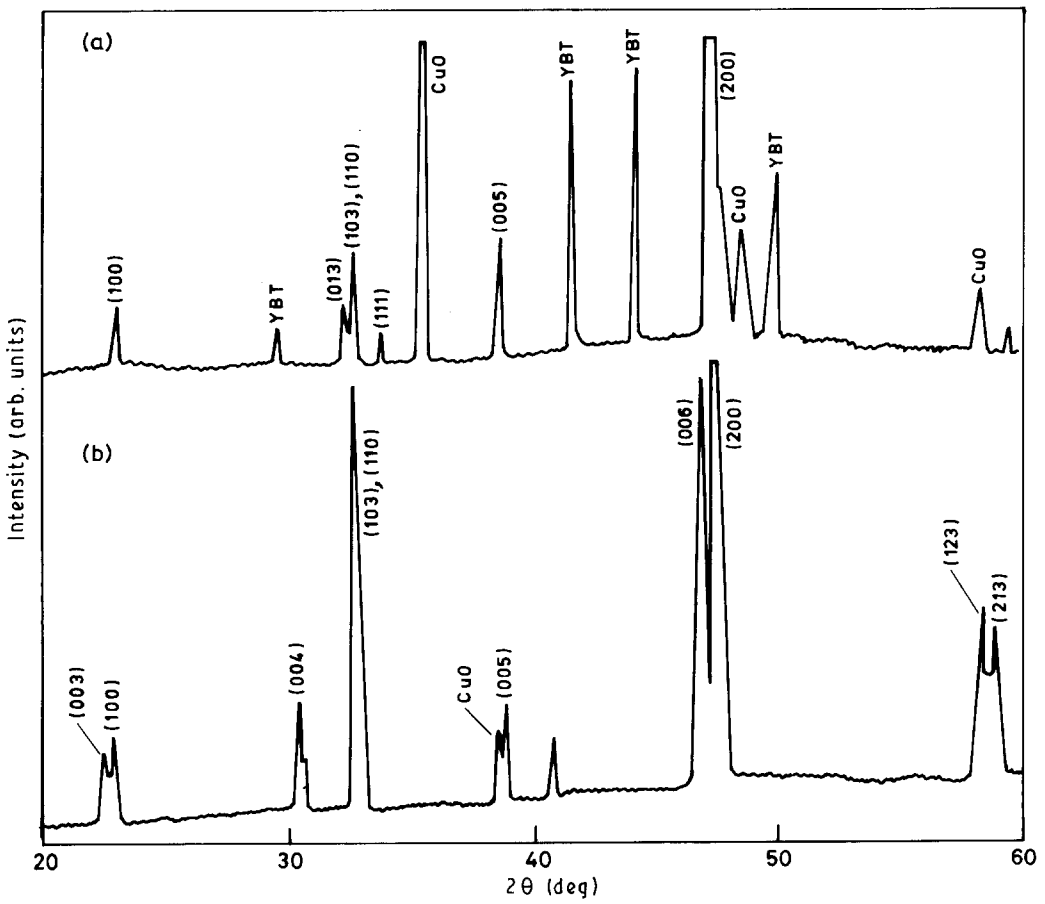

Figure 7 XRD patterns recorded for films on $SrTiO_3$: (a) 2–3 μm and (b) ~15 μm thick films. YBT = $YBa_3Ti_2O_{8.5}$.

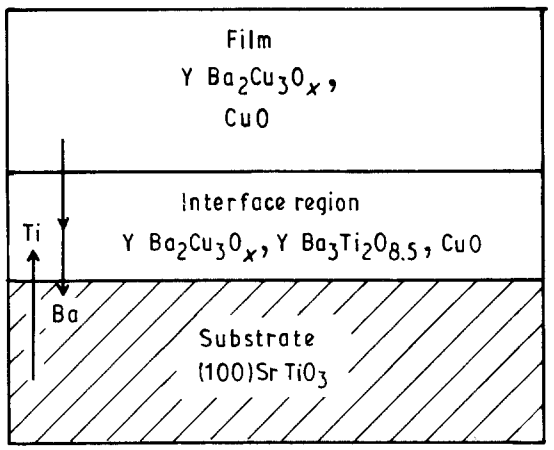

Figure 8 Schematic diagram giving the compositions of the different regions of a film on $SrTiO_3$.

Yttrium diffusion and the formation of YAG have been seen by us to become enhanced when the processing temperature exceeds 1000 °C, while the formation of Al_2BaO_4 is predominant when the film processing temperature is maintained below 1000 °C.

3.3. $SrTiO_3$ substrate

The results of EDAX for as-prepared and partially etched films have been given in Table I. For a fully etched film this analysis would not be possible due to the energy overlap of the characteristic X-rays emitted from Ba and Ti. From the results of Table I, the diffusion of Ba from the film towards the substrate is clearly evident here. For the interface region, the XRD recorded is shown in Fig. 7a. The results show the presence of the orthorhombic phase of 123, CuO and in addition reflections corresponding to d spacings of 0.2994, 0.2191, 0.2082 and 0.1832 nm are also observed. These reflections are found to match those due to $YBa_3Ti_2O_{8.5}$ [14]. As would be expected, such films exhibit a metallic behaviour in the normal state but have poor superconducting transition temperatures as shown in Fig. 2b. In contrast, in the XRD recorded for a thick film and as shown in Fig. 7b, the predominant formation of 123 phase with grains oriented along a and c axes is observed. As a result of the reaction between the substrate and the film constituents, the compositions for different regions of the film obtained are as shown in Fig. 8. It is clear from this that the reaction at the interface leads to a situation as if the diffusion of Ba from the bulk of the film towards the interface has taken place.

3.4. MgO substrate

The results of the EDAX measurements as summarized in Table I show that the film composition remains more or less unaffected, suggesting insignificant reaction at the interface. The XRD recorded for the interface region is shown in Fig. 9, which supports the above view. While no reaction could be detected, a significant change in the R versus T plot is noted here. As shown in Fig. 1d, the superconducting transition

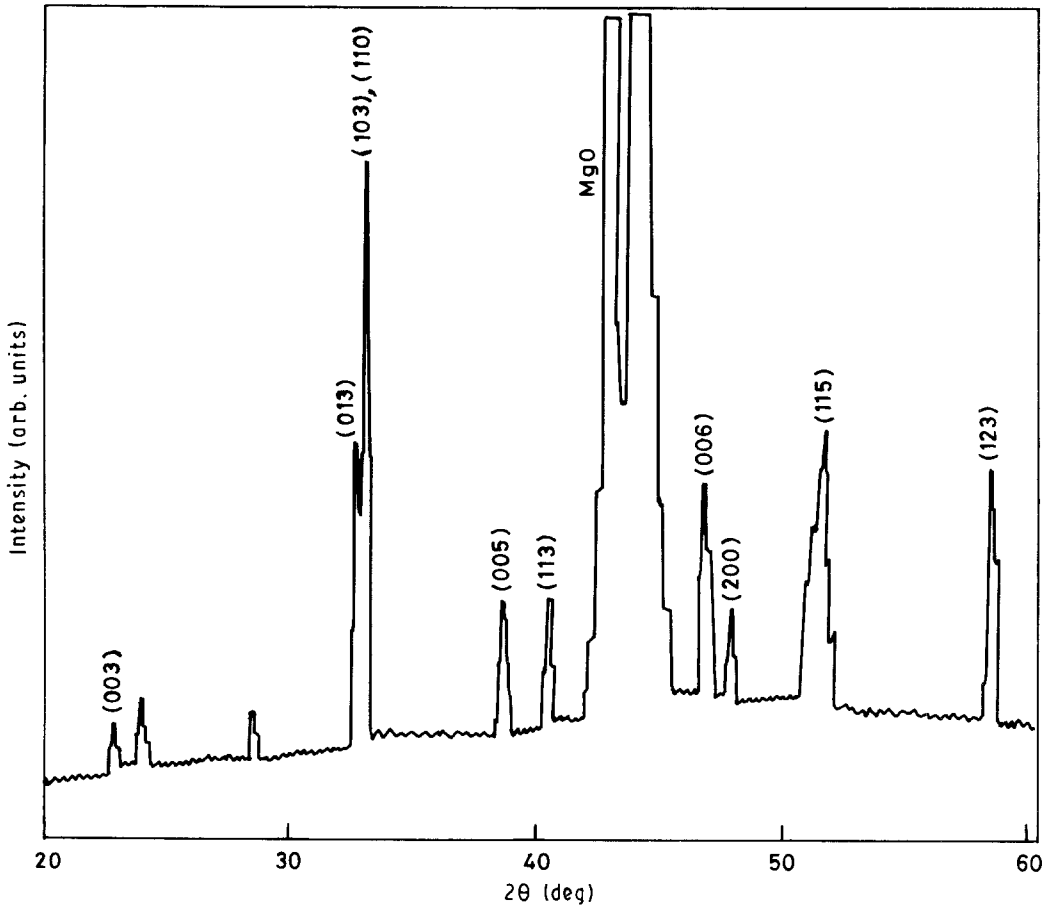

Figure 9 XRD pattern of a 2–3 μm film on MgO.

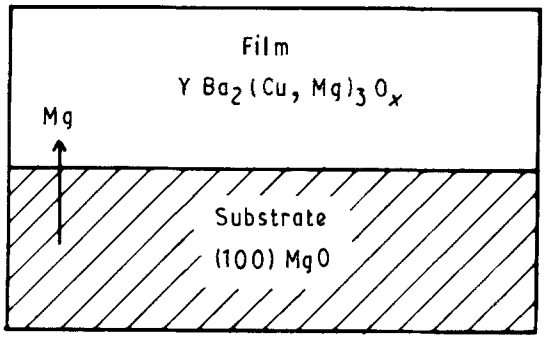

Figure 10 Schematic diagram showing different regions of a film on MgO and their compositions.

temperature, is drastically lowered. The result that no detectable reaction between 123 and MgO takes place is in agreement with earlier reports [4, 15, 16]. The lowering of T_c in the present case is understood in terms of the diffusion of Mg ions from the substrate into the film. The detrimental effect of Mg ions on the superconducting properties of 123 has also been reported by others [17–19]. On diffusing, Mg ions possibly replace the planar Cu ions in 123 because of their nearly equal ionic radii and identical charge. The compositional diagram as suggested by the results is shown in Fig. 10.

3.5. YSZ substrate

The EDAX results as given in Table I clearly show the diffusion of Ba towards the interface. The XRD recorded for the interface region and that of an as-prepared film are shown in Fig. 11. The formation of $BaZrO_3$ is clearly seen and also the reflections due to CuO and Y_2BaCuO_5 are present. The formation of $BaZrO_3$ in this case has also been reported in the literature [3, 4, 20–23]. The compositional diagram based on the data obtained is shown in Fig. 12. A partially etched film as shown in Fig. 2d undergoes a superconducting transition around 64 K. For an as-prepared film, T_c equal to 89 K is obtained from the R versus T plot shown in Fig. 1e.

3.6. Film morphology

The scanning electron micrographs for the films recorded are shown in Fig. 13. It may be seen that all the films except those on Si are quite dense. From this result, a liquid-assisted growth may be inferred in all cases except for films on Si. This result may be understood as follows. It has been demonstrated that in the case of 123 at least two liquid-forming processes below 965 °C take place under an oxygen atmosphere [7]: a eutectic reaction (e_1) at ~925 °C

$$YBa_2Cu_3O_x + BaCuO_2 + CuO \rightleftharpoons \text{liquid}$$

and a peritectic decomposition reaction (p_1) at ~962 °C

$$YBa_2Cu_3O_x + CuO \rightleftharpoons Y_2BaCuO_5 + \text{liquid}$$

In addition to these, at ~1030 °C incongruent melting (m_1) of 123 also takes place in the oxygen atmosphere.

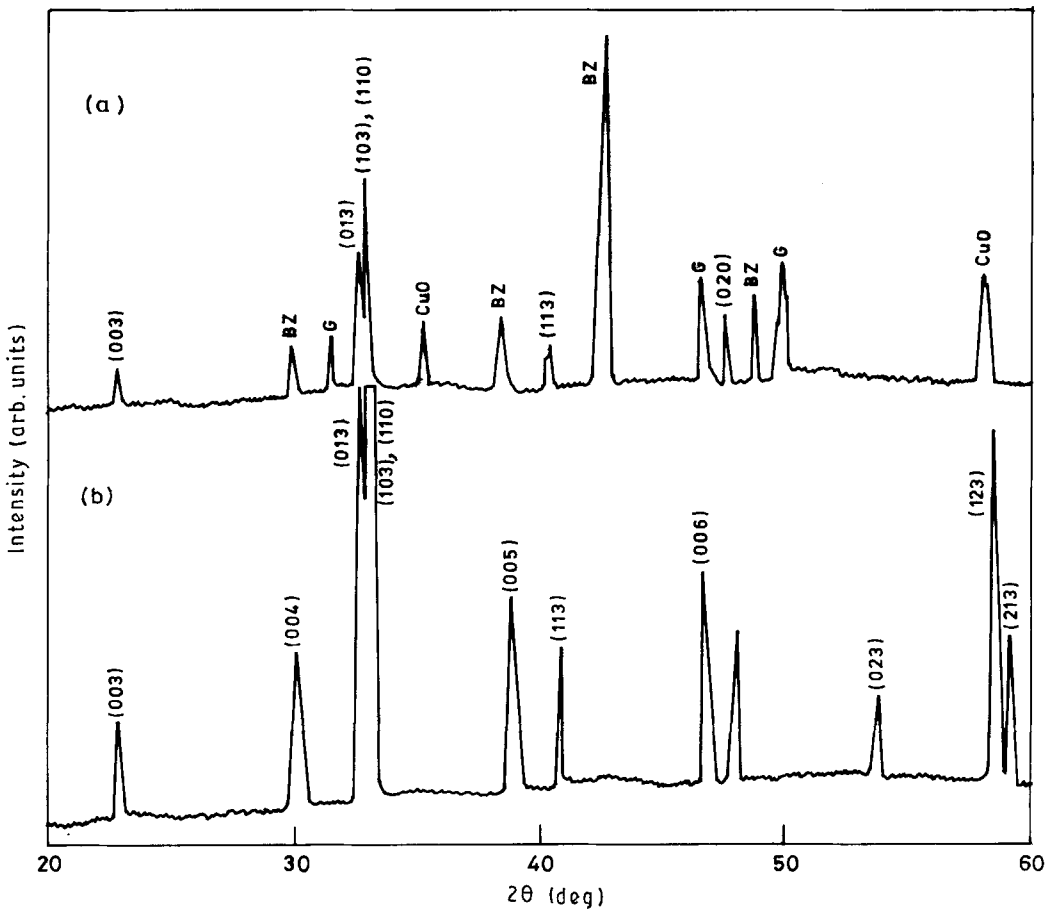

Figure 11 XRD plots for films on YSZ: (a) 2–3 μm and (b) ~15 μm thick films. G = Y_2BaCuO_5, BZ = $BaZrO_3$.

Referring to Fig. 6, it is found that the top of a film on Al_2O_3 is rich in $BaCuO_2$ which suggests the possibility of the e_1 reaction whereby a liquid-assisted growth occurs. In the case of films on $SrTiO_3$ and YSZ, one of the products of the film–substrate reaction is CuO. As has been shown above, the interface region extends to about 3 μm thickness, which means that a large amount of CuO gets released during the film annealing. This suggests the onset of p_1 reaction and again a liquid-assisted growth. A similar situation in the case of MgO-based films is envisaged because of the substitution of Mg ions for Cu in 123 and the consequent release of CuO. In the case of Si-based films CuO is also one of the products of film–substrate reaction; however, as discussed above, a thick buffer

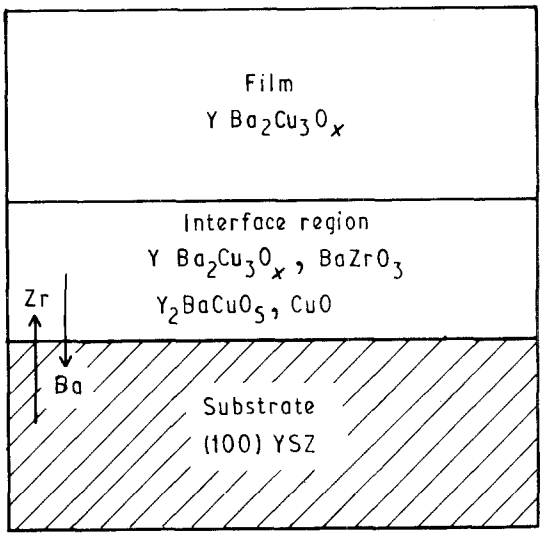

Figure 12 Schematic diagram showing different film regions and their compositions for a film on YSZ.

TABLE II Values of the orientation factor (f) and c parameter calculated for films on different substrates

Substrate	f	c (nm)	T_c (K)
Si	–	1.1681	89.5
Al_2O_3	0.68	1.1752	85
$SrTiO_3$	0.96	1.1684	87.5
MgO	0.23	1.1718	66
YSZ	0.32	1.1682	89

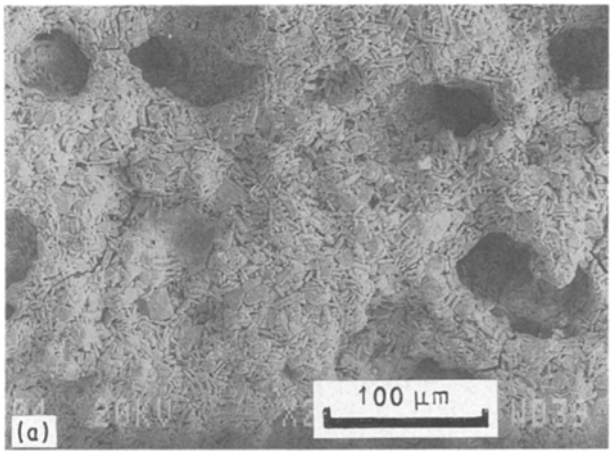

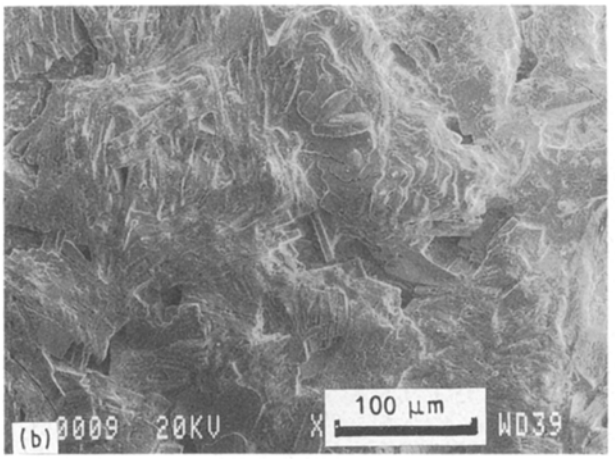

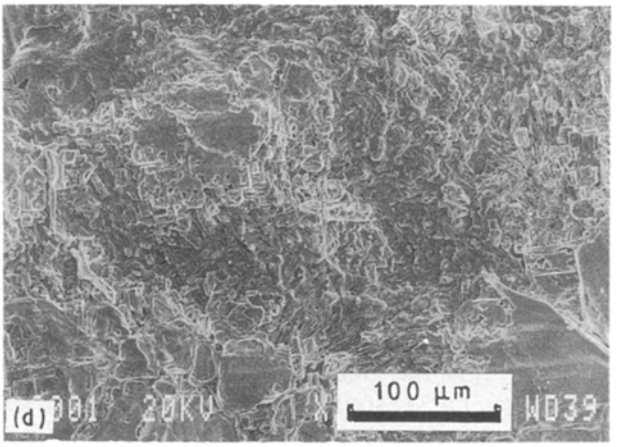

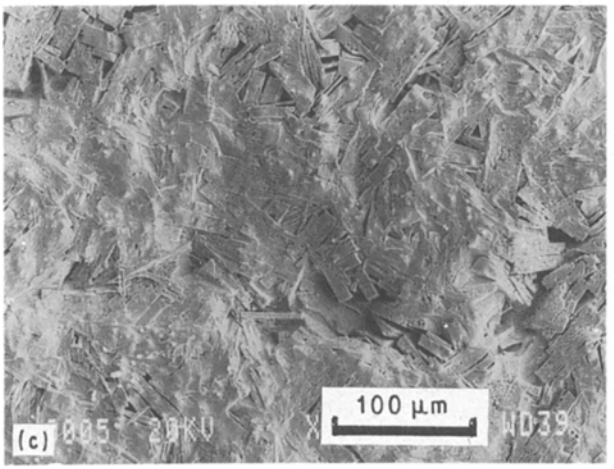

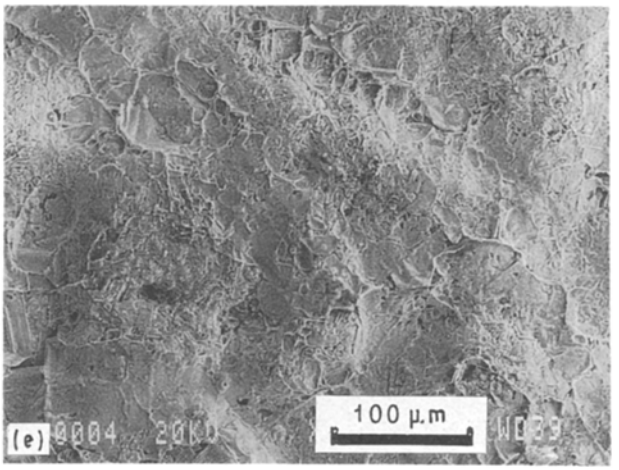

Figure 13 Scanning electron microphotographs for films on (a) Si, (b) alumina, (c) $SrTiO_3$, (d) MgO and (e) YSZ.

layer of Y_2BaCuO_5 separates the CuO from the film. The copper oxide formed at the interface is not accessible for the liquid-forming process, and hence a liquid-assisted growth cannot take place. This explains why in this particular case films are not as dense as in the other cases. The grain growth here is predominantly due to a solid-state reaction process.

The degree of orientation for a film was assessed from its orientation factor f [24]. The values of the f parameter computed for different films are summarized in Table II. It is seen that the films on $SrTiO_3$ are the most oriented ones whereas those on alumina are the next best ones. On the other hand films on Si, as would be expected, are found to have the worst grain orientation. A correlation between the SEM and the f values computed for the respective cases show that the film orientation, besides other factors, is strongly dependent upon the liquid phase available during the annealing.

From the XRD plots recorded for films on various substrates, the average lattice parameter c for the (0 0 1) oriented grains was computed [25]. The results obtained are given in Table II. It is seen that the c parameter is found slightly increased in the case of films on MgO. This is in agreement with the observations reported by others [19]. The reason for the increase in the c parameter for films on alumina substrates is not very clear. It might be due to the partial substitution of Ba at the Y sites. This inference is based on our observations that the films in this case are rich in barium. Support for this view also comes from recent investigations which show the occurrence of cationic disorders in Ba-rich films of 123 material [26]. However, other experiments are needed to confirm/dispute this point of view.

4. Conclusions

The formation of Ba_2SiO_4 and $BaZrO_3$ at the interfaces of Si and YSZ, respectively, and that of Ba_2AlO_4 in the case of Al_2O_3, is observed to take place at comparatively lower temperatures. This result suggests poor stability of 123 with respect to barium. This might be due to the highly electropositive nature of the Ba ions. The other film element diffusing most extensively into the substrates is found to be copper. The superconducting properties of the interface formed in these cases are determined by the amount of new phases formed. In the case of Si, 123 at the interface is seen to completely dissociate into Y_2BaCuO_5, Ba_2SiO_4 and CuO. As a result of this the interface becomes electrically insulating. While Si is found as one of the substrate materials reacting most with 123, YSZ on the other hand is the most stable among the materials investigated. In the case of $SrTiO_3$, the formation of $YBa_3Ti_2O_{8.5}$ at the interface shows that Cu is replaced by Ti. A similar situation in the case of MgO is also noted where Cu in 123 is replaced by Mg ions.

References

1. D. K. ASWAL, S. K. GUPTA, A. K. DEBNATH, G. P. KOTHIYAL, S. C. SABHARWAL and M. K. GUPTA, *Supercond. Sci. Technol.* **4** (1991) 188.
2. X. M. LI, Y. T. CHOU and C. L. BOOTH, *J. Mater. Sci.* **26** (1991) 3057.
3. T. KOMATSU, O. TANAKA, K. MATUSITA, M. TAKATA and T. YAMASHITA, *Jap. J. Appl. Phys.* **27** (1988) L1025.
4. C. T. CHUENG and E. RUCKENSTEIN, *J. Mater. Res.* **4** (1989) 1.
5. M. GURUVITCH and A. T. FIORY, *Appl. Phys. Lett.* **51** (1987) 1027.
6. H. NAKAJIMA, S. YAMAGUCHI, K. IWASAKI, H. MORITA, H. FUJIMORI and H. FUJINO, *ibid.* **53** (1988) 1437.
7. J. E. ULLAMANN, R. W. McCALLUM and J. D. VERHOEVEN, *J. Mater. Res.* **4** (1989) 752.
8. R. S. ROTH, K. L. DAVIS and J. R. DENNIS, *Adv. Ceram. Mater.* **2** (3B) (1987) 303.
9. K. G. FRASE, E. G. LININGER and D. R. CLARKE, *J. Amer. Ceram. Soc.* **70** (1987) C-204.
10. T. VENKATESON, E. W. CHASE, X. D. WU, A. INAM and C. C. CHANG, *Appl. Phys. Lett.* **53** (1988) 243.
11. R. C. BUDHANI, S. H. TZENG, H. J. DOERR and R. F. BUNSHAH, *ibid.* **51** (1987) 1277.
12. N. P. BANSAL, R. N. SIMON and D. E. FARREL, *ibid.* **53** (1988) 603.
13. M. SACHHI, F. SIROTTI, B. MORTEN and M. PRUDENZIATI, *ibid.* **53** (1988) 1110.
14. W. P. T. DERK, H. A. M. VANHALL and C. LANGRIES, *Physica C* **156** (1988) 62.
15. L. A. TIETZ, B. C. CARTER, D. K. LATHROP, S. E. RUSSEK, R. A. BURHAMAN and J. R. MICHEAL, *J. Mater. Res.* **4** (1989) 1072.
16. P. MADAKSON, J. J. CUMO, D. S. YEE, R. A. ROY and G. SCILLA, *J. Appl. Phys.* **63** (1988) 2046.
17. S. J. GOLDEN, H. ISOTALO, M. LANHAM, LANGE and M. RUHLE, *J. Mater. Res.* **5** (1990) 1605.
18. A. FARTASH, I. V. SCHULLER and J. PEARSON, *J. Appl. Phys.* **67** (1990) 2524.
19. M. F. YAN, W. W. RHODES and P. K. GALLAGHER, *ibid.* **63** (1988) 821.
20. Y. MATSUOKA, E. BAN, H. OGAWA and A. SUZUMURA, *Supercond. Sci. Technol.* **4** (1991) 62.
21. J. TABUCHI and K. UTSUMI, *Appl. Phys. Lett.* **53** (1988) 606.
22. S. W. FILIPCZUK, *Physica C* **173** (1991) 1.
23. M. J. CIMA, J. S. SCHNEIDER, S. C. PATERSON and W. GOBLENZ, *Appl. Phys. Lett.* **53** (1988) 710.
24. A. BAILEY, G. ALVAREZ, C. J. RUSSEL and K. N. R. TAYLOR, *Cryogenics* **30** (1990) 599.
25. M. ECE, R. W. VOOK and J. P. ALLEN, *J. Mater. Res.* **6** (1991) 252.
26. V. MATIJASEVIC, P. ROSENTHAL, K. SINOHARA, A. F. MARSHALL, R. H. HAMMOND and M. R. BEASLEY, *J. Mater. Res.* **6** (1991) 682.

Received 21 October 1991
and accepted 30 March 1992